Precise Microstructure Control in Poly(hydroxybutyrate-*co*-lactic acid) Copolymers Prepared by an Yttrium amine bis(phenolate) Complex

Rachel H. Platel and Alexandra R. Hurst*

Department of Chemistry, Lancaster University, Lancaster, LA1 4YB, United Kingdom.

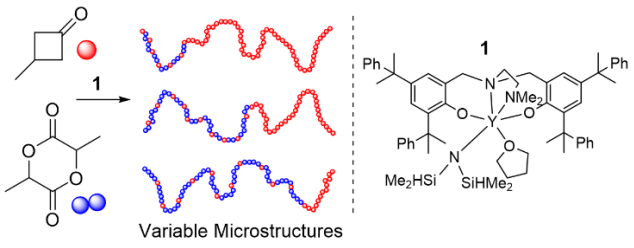

For Table of Contents Use Only

Abstract

A diamino-bis(phenolate) yttrium amide complex, **1**, was used as an initiator in the ring-opening copolymerization of *rac*-lactide (*rac*-LA) and *rac*-*β*-butyrolactone (*rac*-*β*-BL) in toluene at ambient temperature. Copolymers were prepared across a wide composition range (10 – 89% LA content) and the copolymer composition closely matched the monomer feed ratio. The copolymers

had T_g values ranging from 3.8 °C (for a copolymer with 10% LA content) to 44.0 °C (for a copolymer with 89% LA content). T_m ranged from 132 – 144 °C for copolymers with LA composition 48 – 10%. The copolymer microstructure was determined using ^{1}H and $^{13}C\{^{1}H\}$ NMR spectroscopy of copolymers and through reaction monitoring by NMR spectroscopy. This revealed that no BB diads are formed in the copolymer in the presence of any *rac*-LA monomer, even at very high concentrations of *rac*-*β*-BL. However, when [LA] = 0, *rac*-*β*-BL is rapidly polymerized. The copolymers thus have a microstructures consisting of two distinct regions, one containing both LA and BL units in an even distribution and one solely BL or LA units, depending on the monomer feed ratio.

Introduction

The last two decades have seen a surge of interest in biodegradable polymers and copolymers as concern increases about the use of non-renewable resources in plastics and the persistence of plastic waste. Poly(lactic acid) (PLA) is one such material and is currently produced commercially,[1] with uses ranging from packaging[2] to biomedical[3] and agricultural applications.[4] It derives from lactic acid, which can be produced by microbial fermentation of carbohydrates.[5] The most convenient route to PLA (and the one used commercially) is *via* the metal-initiated ring-opening polymerization (ROP) of lactide (LA), the cyclic dimer of lactic acid.[6–8] The stereocentre in lactic acid means that LA can exist as the (*R*,*R*)-, (*S,S*)-, or (*R*,*S*)- isomer, with *racemic*-lactide (*rac*-LA) being a 1:1 mixture of (*R*,*R*)-LA and (*S,S*)-LA.[5] This presence of a stereocentre means there is the potential for control of polymer tacticity through judicious design of the metal initiator.[9–11] The properties of PLA can be markedly improved through formation of

stereocomplexed material,[12,13] although properties such as low melt strength and poor gas barrier properties limit its general applicability.

Poly(hydroxyalkanoate)s (PHAs) are another family of thermoplastic polyesters, the most common of which is poly(3-hydroxybutyrate) (P3HB). Naturally occurring P3HB is produced by bacteria and algae.[14–16] It is a fully isotactic, highly crystalline material with a high melting temperature (180 °C), which has been proposed as a sustainable alternative to isotactic poly(propylene) due to similarities in some mechanical properties. However, it is very brittle and its decomposition temperature is close to the melting temperature, which makes processing a problem.[14] A convenient alternative route to P3HB is the metal-initiated ROP of *rac*-*β*-butyrolactone (*rac*-*β*-BL), a 4-membered lactone. Since this monomer contains a stereocentre it again offers the opportunity for stereocontrol in the polymerization, to produce either isotactically or syndiotactically enriched polymer as opposed to atactic material.[11]

Yttrium and lanthanide amine bis(phenolate) complexes have been extensively explored in the homopolymerizations of *rac*-LA,[17–30] and *rac*-*β*-BL[30–32] and related 4-membered lactones.[19,33,34] This family of complexes, and, in particular, the yttrium analogues, have been shown to exert exceptional stereocontrol in polymerization reactions, generally producing highly heterotactic PLA and syndiotactic P3HB.[35] In addition, they are able to mediate reactions in a controlled manner, producing polymers with predictable molecular weights, based on the monomer to initiator ratio, and very narrow dispersities. Use of a chain transfer agent enables the polymerizations to be immortal, without loss of molecular weight control or stereocontrol.[36–38]

Whilst control over polymer tacticity offers an attractive route to tailor polymer properties, there are limits to the range of properties that can be accessed. Another method to control and modify the mechanical and thermal properties of polymers is by copolymerization of two or more

monomers. This enables the combination of monomers whose constituent homopolymers have very different properties to prepare a copolymer with the most desirable of each homopolymer's properties. Properties can then be tailored by variation of composition and monomer sequence, as well as tacticity and molecular weight. Block, gradient and random/statistical copolymers are all possible and have the potential to exhibit different properties for the same monomer combination. There are relatively few examples reported of the copolymerization of *rac*-LA and *rac*-*β*-BL, especially when compared to other monomer combinations such as *ε*-caprolactone and lactide.[39]

Metal-initiated LA and *β*-BL copolymerization has been reported using complexes incorporating tin,[40] magnesium,[41] aluminium,[42–45] hafnium,[46] indium,[47,48] zinc[49] and copper.[50] One study has been conducted using a salan-supported yttrium complex (salan = *N*,*N*'-dimethyl-*N*,*N*'-bis[(3,5-di-t-butyl-2-hydroxy- phenyl)methylene]-1,2-diaminoethane).[51] Fagerland and co-workers investigated the copolymerization of (*S,S*)-LA, (*R,R*)-LA and *rac*-LA with *rac*-*β*-BL at various temperatures.[43] The conversion of *rac*-*β*-BL was always lower than that of *rac*-LA and kinetic studies showed that the rate of *rac*-LA polymerization was higher than that of *rac*-*β*-BL.

Whilst these studies have highlighted the potential of well-defined metal complexes as single-site initiators of *rac*-LA and *rac*-*β*-BL copolymerizations it is notable that in almost all cases, the reactivity of *rac*-LA is far higher than that of *rac*-*β*-BL, leading to either gradient or blocky microstructures. Additionally, to the best of our knowledge, there have been no reports of the use of yttrium amine bis(phenolate) complexes in the copolymerization of *rac*-LA and *rac*-*β*-BL to date.

In this contribution, we report the copolymerization of *rac*-LA and *rac*-*β*-BL under mild conditions at a range of feed ratios, initiated by an yttrium complex. The microstructure, molecular

weight data and thermal properties of the poly(BL-*co*-LA) copolymers are presented and new ^{13}C NMR assignments for copolymers are proposed. The mechanism of copolymerization is discussed.

Results and Discussion

We were interested in exploring yttrium amine bis(phenolate) derivatives in the copolymerization of *rac*-LA and *rac*-*β*-BL. In particular, given that all previous studies have found that *rac*-LA reactivity is much higher than *rac*-*β*-BL reactivity in copolymerization reactions, we sought an initiator with high activity in *rac*-*β*-BL homopolymerization. The two obvious sites to make structural alterations in amine bis(phenolate) ligands are at the ortho (and para) positions of the phenol groups and the $N(CH_2)_2X$ chelating bridge. It is known that use of $C(CH_3)_2Ph$ groups in the ortho position of amine bis(phenolate) ligands lead to increased rates in *rac*-*β*-BL homopolymerization vs less sterically bulky groups.[52] In *rac*-LA homopolymerization, it has been observed that increasing steric encumbrance around the active metal centre reduces reaction rate.[30] Additionally, it was recently found that the axial NMe_2 bridgehead gave systematically more active initiators than complexes with an OMe bridgehead in the ROP of *rac*-*β*-BL derivatives.[34] Therefore we reasoned that combining these two features (as in **1**) should provide an initiator with enhanced activity in *rac*-*β*-BL ROP vs *rac*-LA ROP and provide copolymer structures that deviated from a blocky microstructure. The strategies of selecting an initiator with high reactivity towards the homopolymerization of the less reactive monomer to enable more favourable competition between monomers in copolymerizations[53] and use of bulky substituents in the coordination sphere of the metal to reduce the coordination ability of LA[54,55] have both been used successfully in LA/ε-caprolactone copolymerizations to favour the formation of statistical copolymers.

Complex **1** was prepared in a protonolysis reaction between ligand H_2L and $Y(N(SiHMe_2)_2)_3(THF)_2$, following a literature procedure (Scheme 1)[30] and characterized by ^1H and $^{13}C\{^1H\}$ NMR spectroscopy. The activity of **1** in the homopolymerization of *rac*-*β*-BL and *rac*-LA ROP has not been previously reported so these reactions were explored first to establish a baseline for copolymerization studies. Reactions were conducted in both THF and toluene in order to determine the best solvent for copolymerization reactions.

Scheme 1: Synthesis of **1**.

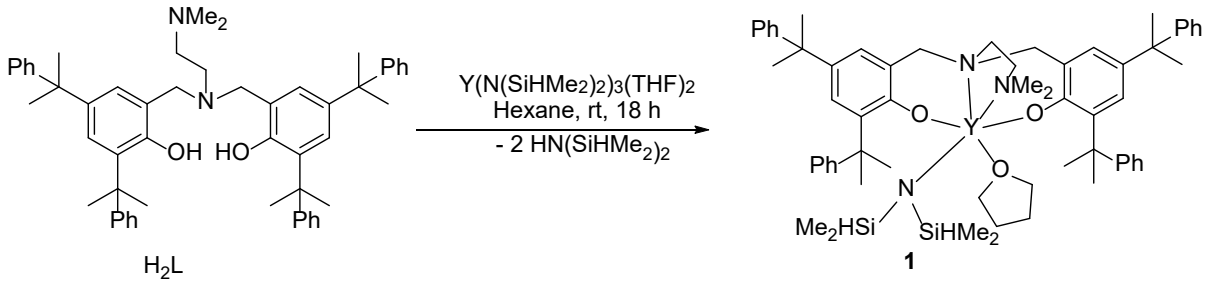

There was a marked difference in activity and stereoselectivity observed for **1** in the polymerization of both monomers in THF and toluene. The conversion of 400 equivalents of *rac*-*β*-BL by **1** in toluene ($[M]_0$ = 2 M) at ambient temperature was complete within 3 min, whilst in THF the same reaction required 16 h to reach just 44% conversion. Similarly, the tacticity of the poly(3-hydroxybutyrate) formed was highly syndiotactic in toluene (P_r = 0.85), with a significant drop in syndiotacticity in THF (P_r = 0.73). These observations are in line with those found previously for other amine bis(phenolate) supported lanthanide complexes,[31,32] and we attribute the lower reactivity in THF to the coordinating solvent competitively coordinating to the metal centre. On the other hand, the polymerization of 200 equivalents of *rac*-LA by **1** ($[M]_0$ = 1 M) at ambient temperature proceeded at similar rates in toluene and THF, requiring 4 h to reach complete conversion. Whilst in THF the polymer formed was almost perfectly heterotactic (P_r = 0.99), in

toluene the polymer only had a slightly heterotactic bias (P_r = 0.60). Again, this large difference in stereoselectivity has previously been reported for similar initiator systems[23] and is believed to arise due to THF coordinating to the metal centre. Due to the very large difference in reactivity of *rac*-*β*-BL with **1** in THF vs toluene, it was decided to use toluene as the solvent for copolymerization reactions. However, the solubility of *rac*-LA in toluene is much lower than in THF. Consequently, some of our studies have been conducted in dichloromethane, in which similar behaviour of the monomers to toluene is observed.

ROP reactions were performed in solution on mixtures of *rac*-*β*-BL and *rac*-LA, initiated by **1** at ambient temperature (Scheme 2). A full range of feed ratios were investigated. Quantitative conversion (assessed by ^{1}H NMR spectroscopy of quenched polymerization reactions) of 400 equivalents of monomer was achieved in all cases within 4 h for $[M]_0$ = 2 M. The time required to reach full monomer conversion increased as the ratio of *rac*-LA increased; ranging from 30 min for *β*-BL:LA = 90:10 to 4 h for *β*-BL:LA = 10:90. These times are in line with those found for homopolymerizations and underline the high activity of **1** as an initiator in *rac*-*β*-BL ROP. After work-up the polymers were dissolved in the minimum volume of chloroform and precipitated from cold methanol. Crude yields were generally >90% and yields after precipitation ranged from 47-98%. Some of the copolymers adhered to the filter paper during precipitation, meaning not all polymer could be recovered. This accounts for the low yields in some cases. We confirmed through work-up of the filtrates that significant amounts of soluble polymer fractions were not being lost through the precipitation process.

Scheme 2: Ring-Opening Copolymerization of *rac*-*β*-BL and *rac*-LA initiated by **1**.

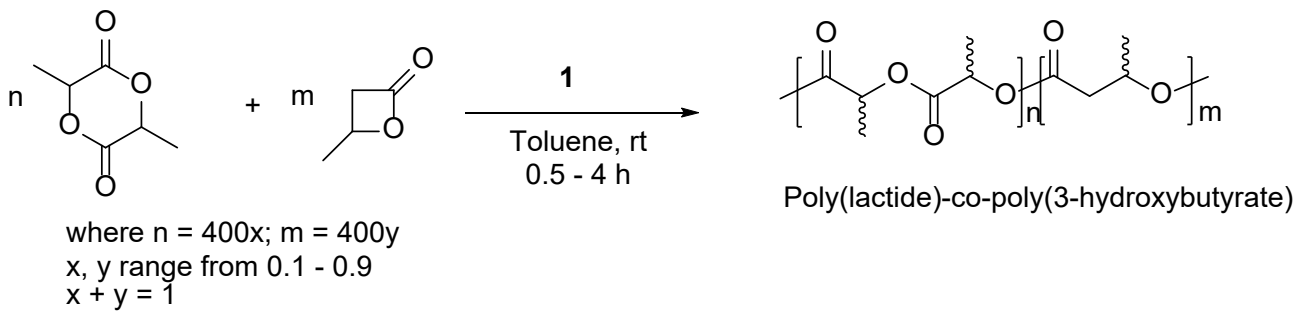

The microstructures of the copolymers obtained were determined using ^{1}H and $^{13}C\{^{1}H\}$ NMR spectroscopy. The ^{1}H NMR spectrum was assigned according to previous literature reports (a typical spectrum is shown in Figure 1).[40,43] The molar composition of the poly(BL-*co*-LA) copolymers was determined by relative integration of the methylene CH_2 signal of BL units and the methine signals of both BL and LA units (where LA refers to a "lactate" unit, -$OCH(CH_3)C(O)$-, i.e. half a LA monomer; BL refers to a butyrate unit, -$OCH(CH_3)CH_2C(O)$, Table 1). The polymer composition matched the feed ratio very closely indeed, showing that **1** is a rapid and efficient initiator for the copolymerization of mixtures of *rac*-*β*-BL and *rac*-LA to full conversion. The ^{1}H NMR spectrum also allows for determination of the percentage of BB homodiads and BL heterodiads (where BB refers to a BL unit adjacent to another BL unit; BL refers to a BL unit adjacent to a LA unit), by comparison of the integrals of the BL unit methylene signals. A multiplet centred around 2.75 ppm arises from BL diads whilst another centred at 2.46 is due to BB diads.[40,43] Up to a composition of 50% LA in the copolymer, the percentage of heterodiads approximately matches the molar percentage of LA units in the polymers. Then, for LA ≥ 70% there are no BB homodiads detected by ^{1}H NMR in the copolymers, i.e. all BL units lie next to a LA unit. The fact that there are heterodiads present in the spectra of all copolymers also confirms that copolymerization, rather than homopolymerization, has occurred.

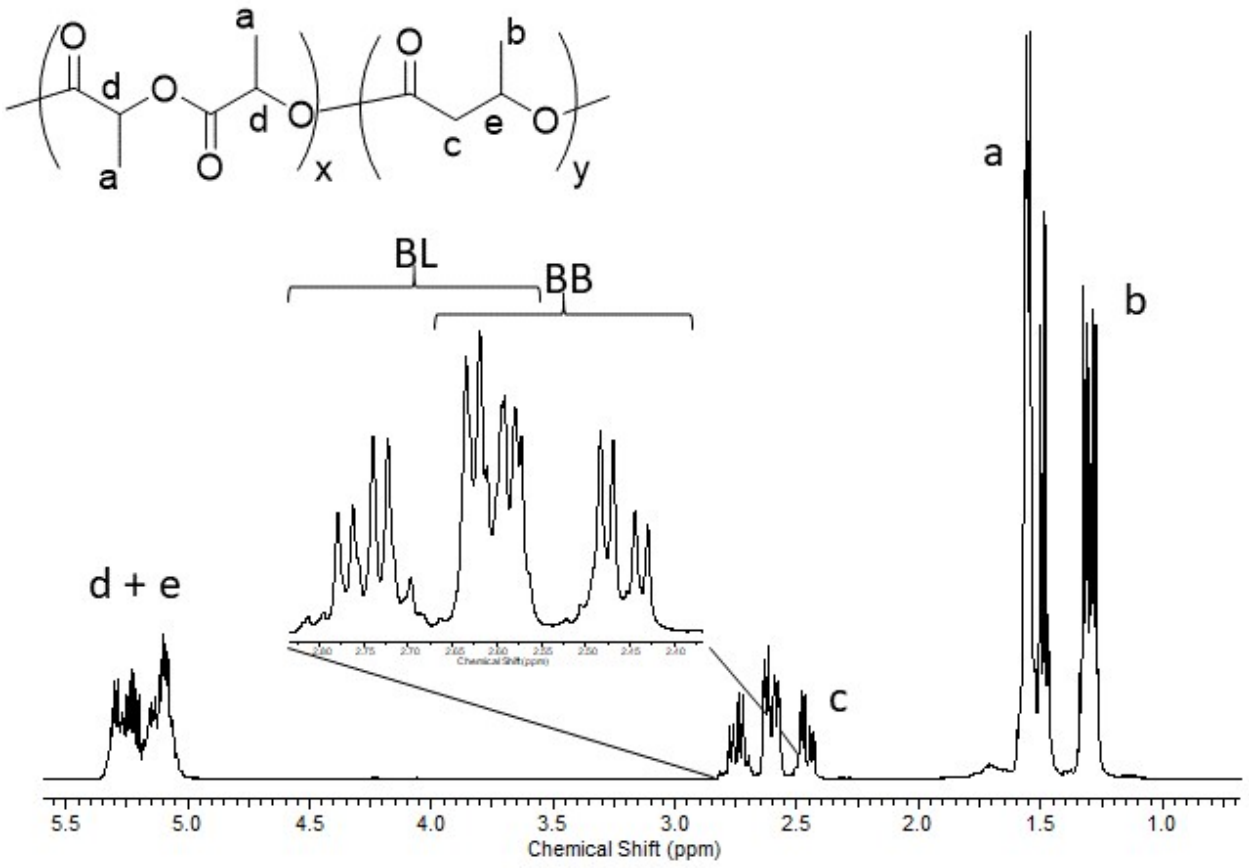

Figure 1: ^{1}H NMR spectrum (400 MHz) of a poly(BL-*co*-LA) copolymer (52% BL molar composition) in $CDCl_3$ showing the assignment of signals.

Table 1. Microstructural Data for the Ring-Opening Copolymerization of *rac*-*β*-BL and *rac*-LA initiated by **1**.[a]

Entry	LA:BL molar feed ratio	Polymer composition (LA:BL molar ratio)[b]	Ratio of BL:BB diads[b]	Triad Ratios[c]			
				BLL	LLL	LLB	XBX[d]
1	10:90	10:90	10:90	7	0	15	78
2	20:80	20:80	18:82	15	7	22	57
3	30:70	29:71	26:74	22	8	28	42

4	40:60	39:61	40:60	26	10	37	27
5	50:50	48:52	54:46	34	14	35	17
6	60:40	61:39	83:17	40	17	40	3
7	70:30	67:33	100:0	43	20	37	0
8	80:20	77:23	100:0	48	26	26	0
9	90:10	89:11	100:0	55	35	10	0

[a] Reaction conditions: Total monomer amount of 4 mmol in toluene (2 mL) at room temperature, with $([BL]_0 + [LA]_0)/[Y] = 400$. Reaction time 1 h. [b] Determined from ^{1}H NMR spectra. [c] Determined from ^{13}C NMR spectra.[40] [d] B<u>B</u>B+B<u>B</u>L+L<u>B</u>B+L<u>B</u>L

Quantitative $^{13}C\{^1H\}$ NMR spectra of the copolymer samples gave greater insight into the poly(BL-*co*-LA) microstructure. The CO, CH, CH_2 and CH_3 regions of the spectrum contained signals for the relevant C atoms that can be assigned to various diads and triads of BL- and LA-containing sequences, as reported previously (Figure 2),[40] although this contribution used (*R*)-*β*-BL and (*S,S*)-LA. Our spectra were rather more complex, which we attribute to the racemic nature of the monomer pool and the fact that the carbon atoms in both PLA and P3HB are additionally sensitive to the relative stereochemistry of surrounding monomer units to at least a tetrad[56–58] and diad level,[59] respectively. The methine region was the most useful, since the *C*H nuclei are sensitive to their environment at a triad level. Thus, it was possible to identify and compare the integrals of signals arising from B-centred triads (B<u>B</u>B, B<u>B</u>L, L<u>B</u>B, L<u>B</u>L), L<u>L</u>B, L<u>L</u>L and B<u>L</u>L triads (Table 1). Copolymerization reactions were conducted with (*S,S*)-LA in an attempt to simplify the copolymer ^{13}C NMR spectra. However, the ^{13}C NMR spectra for copolymers were identical to those obtained using *rac*-LA across a full range of monomer feed ratios, indicating that some epimerization of the LA monomer was occurring. This persisted in

dichloromethane and was also evident in (*S,S*)-LA homopolymerizations in toluene and dichloromethane. We therefore did not pursue the use of (*S,S*)-LA as a monomer for this study.

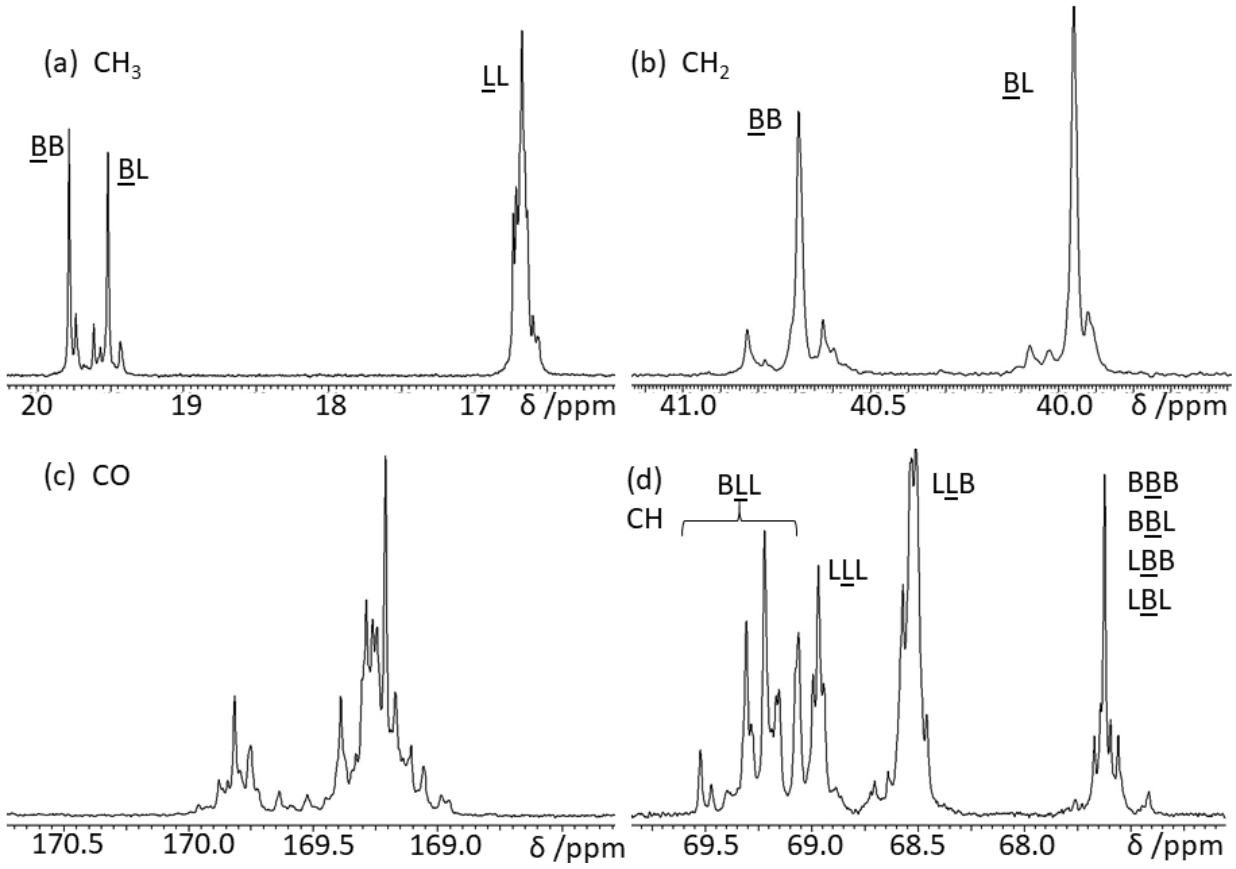

Figure 2: $^{13}C\{^{1}H\}$ NMR spectrum (175 MHz) of a poly(BL-*co*-LA) copolymer (52% BL molar composition) showing the assignment of signals according to literature.[40] The various monomer sequences are labelled at either diad or triad level (L = LA unit, i.e. 0.5 lactide; B = BL unit).

The molecular weights of the polymers were determined by GPC using the MALLS (multi-angle laser light scattering) detection method (Table 2). Each polymer had a monomodal molecular weight distribution, again confirming copolymerization of the monomers. There is a tendency towards lower molecular weights for copolymers with greater proportions of LA. A possible explanation for the low M_n values is the fact that a MALLS detection method was used and a dn/dc

value was calculated for each copolymer. An average dn/dc value, calculated based on the dn/dc values of the constituent homopolymers, was used. However, the particular behaviour of the copolymers in solution could mean these values are inaccurate, which would in turn lead to deviation from theoretical M_n values. Polymer dispersities were low to moderate, ranging from 1.16 – 1.42, compared to values of 1.07 (P3HB) and 1.12 (PLA) for reference homopolymers (Table 2, entries 1 and 9).

Table 2. Molecular Weight Data for the Ring-Opening Copolymerization of *rac*-*β*-BL and *rac*-LA initiated by **1**.[a]

Entry	Polymer composition (LA:BL molar ratio)[a]	Crude Yield (%)	Precipitated Yield (%)	$M_{n\ (Calc)}$[b] /g mol^{-1}	$M_{n\ (Expt)}$[c] /g mol^{-1}	$Đ$[c]
1[f]	0:100	98	*e*	17200	24400	1.07
2	10:90	99	59	36720	36720	1.42
3	20:80	99	83	39040	40250	1.35
4	29:71	96	76	41128	41360	1.41
5	39:61	97	75	43448	39700	1.29
6	48:52	99	69	45536	38950	1.16
7	61:39	78	53	48552	25850	1.26
8	67:33	98	98	49944	31640	1.20
9	77:23	98	47	52264	26430	1.23
10	89:11	93	64	55048	18610	1.42
11[f]	100:0	95	*e*	28800	27700	1.12

[a] Reaction conditions: Total monomer amount of 4 mmol in toluene (2 mL) at room temperature, with $([BL]_0 + [LA]_0)/[Y] = 400$. [b] Determined from ^{1}H NMR spectra. [c] Theoretical number-average molecular weight (M_n), calculated as follows: ((a x 86) + (b x 144))/400, where a = BL molar ratio/100, b = LA molar ratio/100 [d] Experimentally determined number-average molecular weight (M_n) and dispersity ($Đ = M_w/M_n$) determined by GPC-MALLS at 40 °C in $CHCl_3$ using dn/dc values of 0.033 and 0.024 for P3HB and PLA respectively and using dn/dc (copolymer) = (0.033

x BL molar ratio/100) + (0.024 x LA molar ratio/100). [e] Polymer not precipitated. [f] $[Monomer]_0/[Y] = 200$.

The thermal properties of the polymers were determined by differential scanning calorimetry (DSC); a temperature range of -20 – 200 °C was investigated and the results are collected in Table 3. The reference PLA homopolymer prepared from 100% *rac*-LA feed is amorphous, as expected for PLA with a slight heterotactic bias;[60] the reference P3HB homopolymer prepared from 100% *rac-β*-BL feed has a T_m of 150 °C, as expected for highly syndiotactic P3HB.[32] On this basis we deduce that crystallinity in the copolymers arises from BL rich regions. Remarkably, the polymers showed a melting transition up to a 48% molar ratio of LA, although at this composition ΔH_m was just 2.58 J g^{-1}. At LA ratios of 61% and higher, the polymers were amorphous. These copolymers also contain a low percentage of BB homodiads (or none at all), which supports the theory that it is the BL rich regions of the copolymers which are crystalline. Melting temperatures ranged from 132 – 144 °C for copolymers with BL composition 52 – 90%. As the BL content of the copolymer increases, the T_m value also increases, as does the percentage of BB diads in the copolymer. Each thermogram contains a single glass transition temperature (T_g), which increases as the molar percentage of LA in the copolymer increases. The experimental T_g values are in excellent agreement with those calculated using the Fox equation (Figure S60),[61] indicating that the copolymers contain fully compatible blocks and there is no phase separation.

Table 3. Thermal Properties of Poly(BL-*co*-LA) copolymers and reference homopolymers[a]

Entry	Polymer composition (LA:BL molar ratio)[b]	T_g / °C	T_m / °C	ΔH_m / J g^{-1}	T_c / °C	ΔH_f / J g^{-1}
1	0:100	2.4	150.19	34.36	117.72	42.29
2	10:90	3.8	143.86	41.50	111.58	41.65

3	20:80	11.1	140.08	26.14	106.45	26.94
4	29:71	18.4	137.57	20.34	99.64	20.81
5	39:61	23.1	131.77	13.70	78.90	10.75
6	48:52	26.5	132.13	2.58	-	-
7	61:39	32.3	-	-	-	-
8	67:33	34.0	-	-	-	-
9	77:23	36.1	-	-	-	-
10	89:11	44.0	-	-	-	-
11	100:0	41.3	-	-	-	-

[a] Determined from DSC. All T_m and T_g values were obtained from the 2nd heating scan; T_c values were obtained from the 1st cooling scan. The heating rate was 10 °C/min and the cooling rate was 5 °C/min. A blank entry indicates the transition was not detected. [b] Determined from ^{1}H NMR spectra.

The microstructural data collected for each copolymer composition data, and in particular the fact that at a 52% BL composition, 54% of the BL-based diads are heterolinkages, lead us to attempt to determine reactivity ratios for this system, in order to establish whether statistical copolymers were being formed and give a full understanding of the copolymer structure. Copolymerizations at various initial monomer feed ratio were carried out and quenched at low conversions, and the polymer compositions determined. However, both the Fineman-Ross[62] and the Kelen-Tüdõs[63] methods failed to give data that would fit satisfactorily to the derived equations. Therefore, the recently proposed method of Lynd, Beckingham and Sanoja[64] was used. However, this method also gave inconsistent results, with different values for r_{LA} and r_{BL} generated depending on the monomer feed ratio. Taken together, these results show that this copolymerization cannot be described by a nonterminal/ideal model, where the rate of incorporation of each monomer relates purely to the reactivity of each monomer. Rather, they suggest that incorporation rates have a marked dependence on the identity of the chain end.

Therefore, the reaction at various monomer feed ratios were followed over time by ^{1}H NMR spectroscopy, in order to observe monomer consumption over the reaction. Due to the rapid nature of the reactions at $[M]_0$ = 2 M, the reactions were conducted at $[M]_0$ = 0.5 M in order that they could be monitored. We first investigated the $[LA]_0$ = $[\beta\text{-BL}]_0$ = 0.25 M reaction in toluene. Aliquots were removed from the reaction vessel at various time intervals and quenched in $CHCl_3$. After work up, the samples were analysed by ^{1}H NMR spectroscopy. Percent conversion of monomer was determined using 1,3,5-trimethoxybenzene as an internal standard. A plot of conversion vs. time for the ROP of *rac*-LA and *rac*-*β*-BL initiated by **1**, with molar ratio of *rac*-LA: *rac*-*β*-BL = 50:50 is shown in Figure 3. The *rac*-LA is consumed at a faster rate than the *rac*-*β*-BL, reaching 95% conversion after approximately 60 min, at which point the *rac*-*β*-BL has reached 48% conversion. For all samples taken to this point, the *rac*-LA conversion is approximately double the *rac*-*β*-BL conversion. Initially *rac*-*β*-BL consumption follows first order kinetics, but then consumption slows when *rac*-LA conversion ≥80%. Once all the *rac*-LA has been consumed, *rac*-*β*-BL conversion continues to reach >90%. Remarkably, from examination of the ^{1}H NMR spectra of the polymer samples we observed that until all the *rac*-LA has been consumed, there are no BB linkages formed in the copolymer, i.e. the signal at 2.46 ppm in the ^{1}H NMR spectrum is absent.

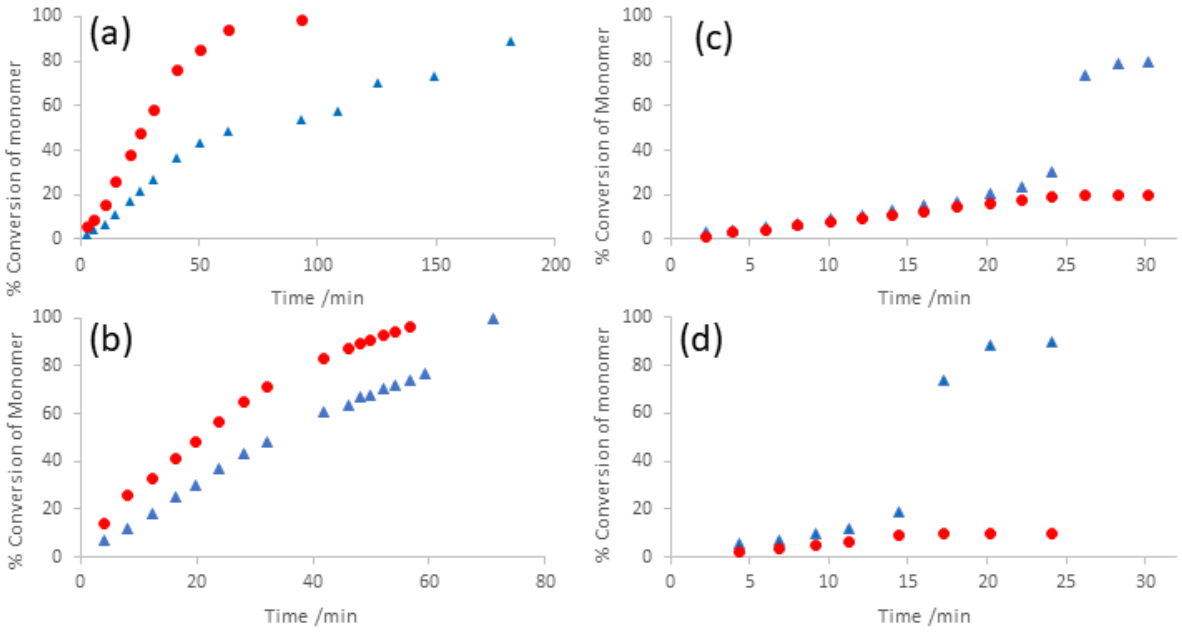

Figure 3: Plots of conversion vs. time for the ROP of *rac*-LA and *rac*-*β*-BL initiated by **1**. *rac*-LA conversion = ●, *rac*-*β*-BL conversion = ▲. (a) *rac*-LA:*rac*-*β*-BL = 50:50 mol%, in toluene, maximum conversion is set to 100% for *rac*-LA and *rac*-*β*-BL; (b) *rac*-LA:*rac*-*β*-BL = 50:50 mol%, in dichloromethane, maximum conversion is set to 100% for *rac*-LA and *rac*-*β*-BL; (c) *rac*-LA:*rac*-*β*-BL = 20:80 mol%, in dichloromethane, maximum conversion is set to 20% for *rac*-LA and 80% for *rac*-*β*-BL; (d) *rac*-LA:*rac*-*β*-BL = 10:90 mol% in dichloromethane, maximum conversion is set to 10% for *rac*-LA and 90% for *rac*-*β*-BL.

From these data we infer that the polymer chains consist of a section comprising 4 times the molar quantity of LA units to BL units, with all BL units surrounded by LA units, and then another well-defined section of 100% BL units. In this case, with a feed ratio of *rac*-LA: *rac*-*β*-BL = 50:50, approximately 50% of the BL units are incorporated into the mixed section, and 50% are in the purely BL section.

To confirm that the microstructure of the mixed portion of the copolymer has a regular structure, rather than a tapered or gradient structure, aliquots were removed from a polymerization reaction

(*rac*-LA: *rac*-*β*-BL = 50:50 mol%) at 15 min, 30 min and 60 min and the polymer samples obtained after work-up analysed by both ^{1}H and ^{13}C NMR spectroscopy. The molar compositions of each copolymer sample (determined from ^{1}H NMR spectroscopy) are 33% BL and 67% LA, indicating composition remains constant until the *rac*-LA reaches full conversion (after 60 min *rac*-*β*-BL is 48% converted and *rac*-LA is 94% converted). Additionally, the microstructure (determined from ^{13}C NMR spectroscopy) is also the same in each of the 3 samples, with an L<u>L</u>B:L<u>L</u>L:B<u>L</u>L/L<u>B</u>L ratio of 1:2:2 (triad assignment is discussed later). This not only supports the theory that the copolymer microstructure in the mixed portion of the copolymer does not change as a function of changing monomer concentrations during the reaction, but also suggests that little to no transesterification occurs under the reaction conditions.

The difference in reactivity between monomers in homo- and copolymerizations (higher activity of *rac*-*β*-BL in homopolymerization) follows what others have observed and reported. The reasons for this difference in reactivity between rac-LA and *rac*-*β*-BL are unclear, but may reflect an ability for the C=O moiety in *rac*-LA to coordinate more strongly to the yttrium centre than the *rac*-*β*-BL C=O.

Due to the low solubility of *rac*-LA in toluene we repeated this experiment in dichloromethane (Figure 3 (b)). In this case the consumption of both monomers is somewhat linear and the reactivity of *rac*-*β*-BL is higher than in toluene, so that at complete conversion of *rac*-LA, *rac*-*β*-BL conversion has reached approximately 75%. Again, relatively rapid consumption of the remaining *rac*-*β*-BL then occurs.

In order to determine how initial monomer concentration influences polymer microstructure, further reactions conducted in dichloromethane were monitored over time, with [*rac*-LA]$_0$:[*rac*-*β*-BL]$_0$ ratios of 10:90, 20:80, 70:30 and 90:10. For the reaction with *rac*-LA: *rac*-*β*-BL = 10:90

mol% ([*rac*-LA]$_0$ + [*rac*-*β*-BL]$_0$ = 0.50 M, Figure 3(d)), both monomers are consumed at similar rates initially (taking into account their different initial concentrations). Thus, despite *rac*-*β*-BL being present in great excess with respect to *rac*-LA, it is incorporated into the copolymer at the same rate as *rac*-LA. After approximately 15 min, all of the *rac*-LA is consumed, at which point the *rac*-*β*-BL conversion increases very rapidly over the next 5 min to reach maximum conversion. The reaction with *rac*-LA:*rac*-*β*-BL = 20:80 mol% ([*rac*-LA]$_0$ + [*rac*-*β*-BL]$_0$ = 0.50 M, Figure 3(c)), tells a similar story, although in this case *rac*-LA conversion does not reach a maximum until 50 min, and *rac*-*β*-BL conversion then increases rapidly between 50 min and 70 min.

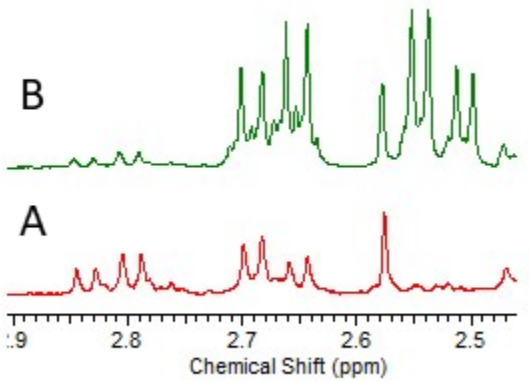

Figure 4: ^{1}H NMR spectra ($CDCl_3$) showing the polymer BL CH_2 signals in samples taken from the ROP of *rac*-LA and *rac*-*β*-BL in toluene initiated by **1**, with *rac*-LA:*rac*-*β*-BL = 10:90 mol%. Signals at 2.82 and 2.66 ppm arise from BL diads and those at 2.66 and 2.53 ppm arise from BB diads. Spectrum A = 20 min and shows no BB homodiads present; Spectrum B = 22.5 min and shows significant BB homodiad formation.

Again, to further probe the microstructure of the copolymer formed when *rac*-LA: *rac*-*β*-BL = 10:90 mol%, and to specifically examine the microstructure of the copolymer formed in the initial stage of the reaction, a polymerization reaction was conducted in toluene and quenched after a

reaction time of 20 min before being examined by ^{1}H and ^{13}C{^{1}H} NMR spectroscopy. The *rac*-LA had reached >98% conversion and the molar composition of the copolymer was 49:51 LA:BL. As expected, there are no BB homodiads present in the copolymer, which, when considered alongside the copolymer composition, indicates that the copolymer has a very highly alternating structure. There is a very low intensity LLL signal in the ^{13}C{^{1}H} NMR spectrum (approximately 17%), indicating a low percentage of LLL triads. To the best of our knowledge, poly(BL-*co*-LA) with this particular microstructure has not previously been prepared *via* an ROP strategy.

Characterization of this copolymer revealed that the methine region of the ^{13}C{^{1}H} NMR spectrum of the copolymer does not contain any signal in the range 67.45-67.75 ppm (previously assigned to BBB, BBL, LBB and LBL sequences).[40] This result lead us to revisit the previously proposed microstructural data. Due to there being confirmed incorporation of *rac*-*β*-BL into the copolymer, and evidence for the presence of BL heterodiads in the ^{1}H NMR of the sample, there must be LBL triad sequences in the copolymer. Indeed, this is the only linkage type centred on 'B' that is expected (^{1}H NMR shows no BB diads). In a report detailing the synthesis of perfectly alternating poly((*S*)-LA-*alt*-(*R*)-3HB) *via* condensation methods, the *C*H resonance of the BL unit (an LBL triad) lies at 68.42 ppm in $CDCl_3$.[65] This indicates that such *C*H environments in our copolymers may have chemical shifts that are closer to 'L' centred triads rather than 'B' centred triads. A combination of ^{1}H–^{1}H COSY, HSQC and HMBC data allowed us to locate the LBL *C*H resonance at 68.54 ppm (Figures S55 – S59). The 2D NMR spectra also suggest that, as well as a signal at 68.97 ppm for the LLL triad, there are resonances at 69.06 and 69.17 ppm which have a purely 'L' contribution. The complexity of the ^{13}C NMR data for these copolymers hinders full assignment of the signals even at high resolution (125 MHz). However, it is possible to extract plausible and self-consistent estimates for ratios of BLL:LLL:LLB/LBL sequences for most of the

copolymers using our proposed peak assignments (Figure 5 and Table 4). The most problematic copolymers are those with high LA content, in which there is significant overlap between the BLL and LLL signals (Figure 5(c)), leading to an overestimation of the proportion of BLL triads and a concomitant underestimation of the proportion of LLL triads, which in turn suggests a negative value for LBL. The percentage of B-containing linkages can be calculated and is close to (within 5%) the copolymer composition (calculated from ^{1}H NMR), further supporting our assignments.

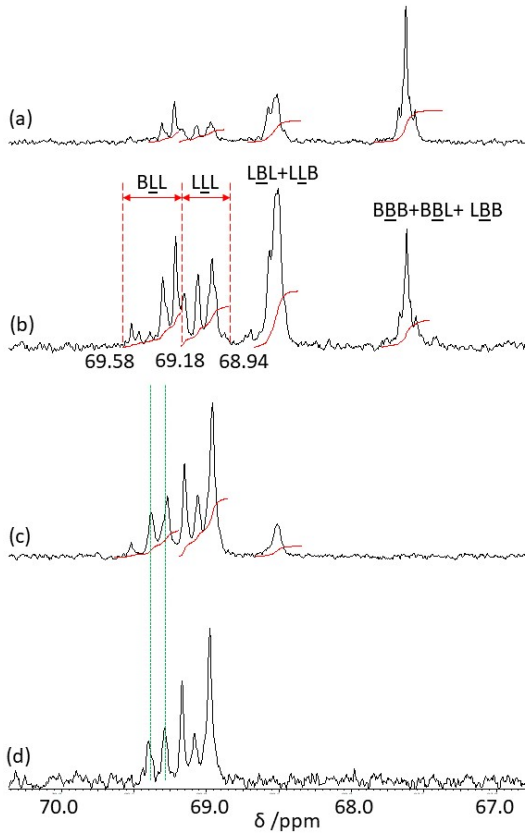

Figure 5: ^{13}C{^{1}H} NMR Spectra of polymers prepared by **1**. (a) Poly(BL-*co*-LA) containing 20% LA; (b) Poly(BL-*co*-LA) containing 48% LA; (c) Poly(BL-*co*-LA) containing 89% LA; (d) PLA. Spectrum (b) shows new triad peak assignments. Dashed lines on (c) and (d) show the presence of LLL signals in the BLL region in copolymers with high LA content.

Table 4: Chemical Shift Ranges and Peak Assignments in the Methine Region of ^{13}C NMR Spectra of Poly(BL-*co*-LA) Samples.[a]

Copolymer LA:BL	% BLL[b]	% LLL[c]	% LBL/LLB[d]	% BBB/BBL/LBB[e]	% LBL[f]	% B-containing linkages[g]
10:90	7	0	15	78	8	93
20:80	9	12	22	57	13	79
29:71	13	17	28	42	15	70
39:61	15	21	37	27	22	64
48:52	22	26	35	17	13	52
61:39	30	27	40	3	10	43
67:33	28	34	38	0	10	38
77:23	27	47	25	0	-[h]	25
89:11	28	61	11	0	-[h]	11

[a]Spectra acquired in $CDCl_3$ at 100 MHz; [b] BLL = $\int 69.58 \longrightarrow 69.18$ ppm in ^{13}C NMR spectrum; [c] LLL = $\int 69.18 \longrightarrow 68.94$ ppm in ^{13}C NMR spectrum; [d] LBL/LLB = $\int 68.75 \longrightarrow 68.45$ ppm in ^{13}C NMR spectrum; [e] BBB/BBL/LBB = $\int 67.80 \longrightarrow 67.40$ ppm in ^{13}C NMR spectrum; [f] LBL = $\int$ LBL/BLL $-$ $\int$ LLB; [g] B-linkages = $\int$ LBL/LLB + $\int$ BBB/BBL/LBB; [h] $\int$ LBL/LLB $-$ $\int$ BLL = negative number.

The copolymerization reaction was investigated in dichloromethane for when *rac*-LA is present in excess. In both cases, the monomer consumption follows pseudo-first order kinetics, and the percentage conversion of *rac*-LA increases more rapidly than of *rac*-*β*-BL. Where *rac*-LA: *rac*-*β*-BL = 90:10 mol%, the *rac*-*β*-BL reaches full conversion before the *rac*-LA is all converted (Figure S48), whereas for the *rac*-LA: *rac*-*β*-BL = 70:30 mol% reaction, both monomers reach full conversion at around the same time (Figure S49). Additionally, there are no BB homodiads observed in the ^1H or ^{13}C NMR spectra of either of the polymers obtained for these monomer ratios (Figures S21, S23, S27 and S29).

For the cases where $[LA]_0 < [\beta\text{-BL}]_0$, the *rac*-LA conversion-time data was compared. Plotting conversion vs. time for a given $[rac\text{-LA}]_0$ gives a straight line up to at least 90% conversion (Figure 6). This data suggests a zero-order dependence on [*rac*-LA] in the rate of copolymerization when $[LA]_0 < [\beta\text{-BL}]_0$. The gradients of the lines are again inversely proportional to $[rac\text{-LA}]_0$; consumption of *rac*-LA occurs at the fastest rate when *rac*-LA:*rac*-*β*-BL = 10:90%. Since the $[rac\text{-BL}]_0$ varies with $[rac\text{-LA}]_0$, the combination of all the data indicates that the rate of insertion of either monomer into the polymer chain is strongly dependent on the concentration of the other monomer.

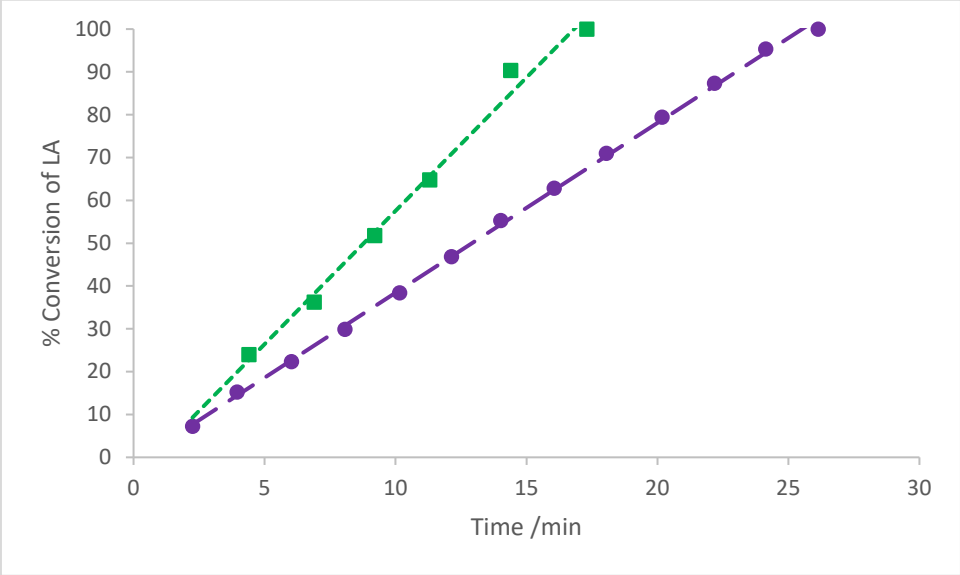

Figure 6: Conversion-time plot for *rac*-LA ROP during the initial stage of the reaction (until [LA] = 0) in *rac*-LA and *rac*-*β*-BL copolymerization initiated by **1**. ■ = LA: *β*-BL 10:90 mol%, k_{obs} = 6.2 min^{-1}, R^2=0.9899; ● = LA: *β*-BL 20:80 mol%, k_{obs} = 4.0 min^{-1} R^2=0.9991.

Taking all the results and observations into account, a mechanism for the copolymerization of *rac*-LA and *rac*-*β*-BL by **1** when $[rac\text{-LA}]_0 < [rac\text{-}\beta\text{-BL}]_0$ is proposed (Figure 7). We propose the rates of polymerization are determined by the following rate constants: k_{BB} = the rate of insertion of *rac*-*β*-BL into Y–BL linkage in the presence of *rac*-LA; k_{LB} = the rate of insertion of *rac*-LA

into Y–BL linkage; k_{LL} = rate of insertion of *rac*-LA into Y–LA linkage; k_{BL} = rate of insertion of *rac*-*β*-BL into Y–LA linkage; k_{BBB} = the rate of insertion of *rac*-*β*-BL into a Y–BL linkage in the absence of *rac*-LA (i.e. once all *rac*-LA has been consumed).

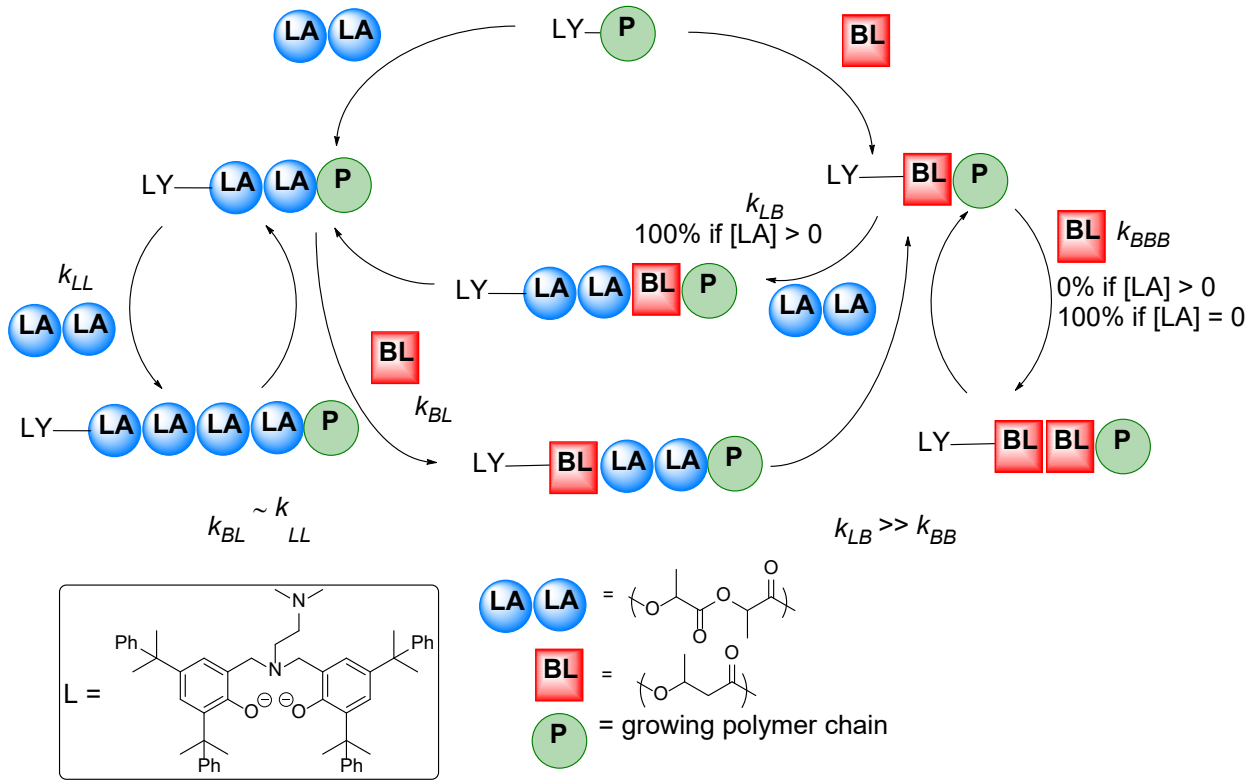

Figure 7: Proposed mechanism of *rac*-LA/*rac*-*β*-BL copolymerization by **1** when $[rac\text{-LA}]_0 \leq [rac\text{-}\beta\text{-BL}]_0$. LA = -OCH($CH_3$)C(O)-, i.e. half a lactide monomer; BL = butyrate unit, -OCH(CH_3)CH_2C(O)-; P = growing polymer chain; k_{BB} = rate of insertion of *rac*-*β*-BL into Y–BL linkage in the presence of *rac*-LA; k_{LB} = rate of insertion of *rac*-LA into Y–BL linkage; k_{LL} = rate of insertion of *rac*-LA into Y–LA linkage; k_{BL} = rate of insertion of *rac*-*β*-BL into Y–LA linkage; k_{BBB} = rate of insertion of *rac*-*β*-BL into a Y–BL linkage in the absence of *rac*-LA.

When *rac*-LA is the last inserted monomer, enchainment of either monomer is possible. The ^{13}C NMR spectra of polymers contains signals attributed to both LLL, BLL and LLB sequences, indicating that either a *rac*-*β*-BL or a *rac*-LA can insert next to a LA unit. For polymers where the

rac-LA feed is 50mol% or lower, the relative integration of these signals (Table 4) shows that the prevalence of –LLLL– sequences (i.e. 2 LA monomers next to each other) and –BLLB– sequences are approximately the same in the polymer chain. This suggests that the rate of *rac*-*β*-BL enchainment into an M–LA linkage (k_{BL}) is similar to the rate of *rac*-LA enchainment into an M–LA linkage (k_{LL}). After enchainment of a *rac*-*β*-BL unit, if *rac*-LA is present then no *rac*-*β*-BL enchainment occurs; thus LA enchainment occurs 100% of the time ($k_{LB} >>> k_{BB}$, since $k_{BB} \approx 0$). Only when [*rac*-LA] reaches 0 is the BB enchainment pathway 'activated' and remaining *rac*-*β*-BL is rapidly consumed ($k_{BB} <<< k_{BBB}$). It is notable that the magnitudes of k_{BBB} and *rac*-*β*-BL homopolymerization appear to be similar, whilst k_{BB} (insertion of *rac*-*β*-BL into an M-BL linkage in the presence of *rac*-LA) is effectively 0. The last enchained monomer dictates which is the next inserted monomer, underlining the nonideal nature of the copolymerization. The fact that the final LLB:LLL triad ratio in copolymers remains constant at ≈ 1:1 for molar feed 80 – 40% for *rac*-*β*-BL, coupled with the fact that the consumption of *rac*-*β*-BL is inhibited when $[rac\text{-}\beta\text{-BL}]_0 > [rac\text{-LA}]_0$ suggests that long sequences of LA units are not formed in the copolymers, except when LA is in great excess. M-BL linkages are regularly formed, which do not then react with the available *rac*-*β*-BL in the reaction mixture if *rac*-LA is present, leading to inhibition of *rac*-*β*-BL enchainment as *rac*-LA is required as the next monomer to be inserted.

Conclusions

In conclusion we have shown that an yttrium amine bis(phenolate) complex can competently mediate the copolymerization of *rac*-LA and *rac*-*β*-BL, producing copolymers with compositions that closely match the monomer feed ratio. Polymers with LA composition of >50% displayed melting temperatures and copolymer T_g values were in agreement with those calculated by the Fox

equation in all cases. This presents the possibility of tuning the copolymer T_m between 132 and 150 °C through variation of the monomer feed ratio.

The novelty of this system lies in the fact that, even with an equimolar amount of each monomer, and taking into account the higher reactivity of *rac*-LA over *rac*-*β*-BL, multiple sequential insertions of *rac*-LA do not occur. Thus, diblock or gradient/tapered copolymer structures, as have been reported by others, are not formed; neither are statistical copolymers. When $[rac\text{-LA}]_0 > [rac\text{-}\beta\text{-BL}]_0$, LA units are present throughout the copolymer, with dispersion of BL units that ranges from even within 50% of the copolymer (at very low $[rac\text{-}\beta\text{-BL}]_0$) to even throughout the copolymer. These copolymers are amorphous. When $[rac\text{-LA}]_0 \leq [rac\text{-}\beta\text{-BL}]_0$, the copolymer microstructure consists of a mixed portion (of homogenous composition) and then a P3HB-only section. The mixed portion ranges in composition from a ratio of LA:BL 2:1 (i.e. -LLBLLBLLB-) when $[rac\text{-LA}]_0$:$[rac\text{-}\beta\text{-BL}]_0$ = 10:90, to a ratio of LA:BL 4:1 (i.e. -LLLLBLLLLBLLLLB-) when $[rac\text{-LA}]_0$:$[rac\text{-}\beta\text{-BL}]_0$ = 50:50. Both the composition of the mixed portion and the length of both sections are determined by the monomer feed ratio, and the length of the P3HB-only section dictates the T_m and crystallinity. The fact that any *rac*-LA at all in the reaction mixture completely supresses the formation of BB linkages, plus the fact that $k_{BL} \geq k_{LL}$ when $[rac\text{-}\beta\text{-BL}]_0 \geq [rac\text{-LA}]_0$, provides a route to precisely control the polymer microstructure and prepare copolymers with complex architectures in a single step.

Experimental Section

The preparation and characterization of **1** and all polymers and copolymers was carried out under an inert (nitrogen) atmosphere using standard Schlenk or glovebox techniques. Dry solvents (toluene, hexane, tetrahydrofuran) were obtained from an Inert SPS (solvent purification system).

All solvents and chemicals were purchased from commercial suppliers (Sigma-Aldrich, Strem, Alfa Aesar, TCI) and used as received except where otherwise specified. *Rac*-LA was recrystallized once from dry toluene and sublimed once under vacuum at 50 °C. *Rac*-*β*-BL was stirred over CaH_2 under N_2 at 50°C overnight, distilled under vacuum and degassed *via* 3 freeze-pump-thaw cycles. C_6D_6 was dried over activated 4 Å molecular sieves and degassed *via* 3 freeze-pump-thaw cycles. 1,3,5-trimethoxybenzene was sublimed under vacuum. The ligand, H_2L,[30] $[Y(N(SiHMe_2)_2)_3(THF)_2]$,[66] and complex **1**[30,34] were prepared following literature procedures.

^1H and ^{13}C NMR spectra were recorded at 400 and 100 MHz, respectively, on a Bruker Avance III 400 MHz spectrometer and referenced to residual solvent peaks. Chemical shifts are reported in ppm and coupling constants in Hz. Selected spectra were recorded at 700 and 125 MHz, respectively, on a Bruker Avance Neo 700 MHz Spectrometer.

Molecular weights of polymers were determined by gel permeation chromatography (GPC) multi-angle laser light scattering (MALLS) in chloroform using a Shimadzu liquid chromatograph equipped with a Shimadzu LC-20AD pump and autosampler, two Phenogel 5 μm linear (2) columns (300 x 7.8 mm), a Shimadzu RID-20A refractive index detector, a Wyatt miniDAWN treos LLS detector and a Wyatt ViscoStar-II viscometer. The column temperature was maintained at 40 °C and the flow rate was 1 mL min^{-1}. Samples were dissolved in chloroform at an approximate concentration of 10 mg mL^{-1}. Data was processed using ASTRA software using dn/dc values of 0.024 and 0.033 for PLA and P3HB, respectively.

Thermal properties of the polymers were determined by differential scanning calorimetry (DSC) using a Mettler Toledo DSC1 STARe instrument equipped with a Julabo FT900 intracooler. Polymer samples of known mass (generally 2-8 mg) were weighed into 40 μL aluminium standard

pans. The sample was heated to 200 °C (at a rate of 10 °C min^{-1}) and held at this temperature for 10 min, before being cooled to -30 °C (at a rate of -5 °C min^{-1}) and held at this temperature for 10 min. The heating and cooling cycles were repeated once, as above. Data was processed using STARe software. T_g and T_m values were taken from the second heating cycle and T_c values were taken from the first cooling cycle.

Representative polymerization Procedure

The required amounts of *rac*-LA and *rac*-*β*-BL (total 4 mmol) were weighed into a vial equipped with a stir bar, to which 1.8 mL toluene was added. A solution of **1** (0.2 mL of a 0.05 M solution, 0.01 mmol) was added *via* syringe to the stirred monomer solution. After 1 h the reaction vial was removed from the glove box and the reaction quenched by the addition of wet hexane. The solvents were removed on a rotary evaporator and a crude ^{1}H NMR spectrum obtained. Purification was achieved by precipitation: the polymer was dissolved in the minimum volume of chloroform (≈ 5 mL) and the resulting solution adding dropwise *via* pipette to 50 mL methanol. The precipitated polymer was collected by filtration under reduced pressure and dried in a vacuum oven at 60 °C overnight. ^{1}H NMR (400 MHz, $CDCl_3$, δ_H, ppm); 5.33 – 5.04 (m, 2H + 1H, C*H* (LA unit) and C*H* (BL unit)), 2.81 – 2.43 (m, 2H, CH_2 (BL unit), 1.57 – 1.47 (m, CH_3 (LA unit)), 1.32 – 1.27 (m, CH_3 (BL unit)); ^{13}C{^{1}H} NMR (100 MHz, $CDCl_3$, δc, ppm); 170.0 – 169.1 (*C*O, LA and BL), 69.7 – 67.8 (*C*H, LA and BL), 41.0 – 40.8 (*C*H_2, BL-BL), 40.1 (*C*H_2, BL-LA), 19.9 and 19.9 (*C*H_3, BL-BL), 19.8 – 19.6 (*C*H_3, BL-LA), 16.8 ((*C*H_3, LA).

Representative polymerization Procedure for kinetic experiments

The required amounts of *rac*-LA and *rac*-*β*-BL (total 4 mmol) were weighed into a vial equipped with a stir bar, to which 6.5 mL toluene was added. A solution of 1,3,5-trimethoxybenzene (0.5

mL of a 0.4 M solution, 0.2 mmol) was added *via* syringe. A solution of **1** (1.0 mL of a 0.01 M solution, 0.01 mmol) was added *via* syringe to the stirred monomer solution. Aliquots of 0.2 mL were taken (by syringe) from the reaction vial at known times, removed from the glovebox and added to chloroform to quench the reaction. The solvents were removed by rotary evaporation to leave a colourless residue which was all dissolved in $CDCl_3$ for ^1H NMR analysis.

ASSOCIATED CONTENT

Supporting Information.

The following files are available free of charge.

^1H and ^{13}C NMR Spectra of **1** and copolymers, GPC traces of copolymers, DSC traces of copolymers, kinetic plots and 2D spectra used in assignment of copolymer ^{13}C NMR spectra.

(PDF)

AUTHOR INFORMATION

Corresponding Author

*E-mail: r.platel@lancaster.ac.uk

Author Contributions

The manuscript was written through contributions of all authors. All authors have given approval to the final version of the manuscript.

Funding Sources

Any funds used to support the research of the manuscript should be placed here (per journal style).

ACKNOWLEDGMENT

The authors thank Dr Geoff Akien for assistance with collecting and interpreting ^{13}C NMR data and Dr David Rochester for assistance with GPC. We are grateful for the use of the Avance Neo 700 NMR spectrometer at University College London and thank Dr Abil Aliev for assistance in data collection.

REFERENCES

(1) Vink, E. T. H.; Davies, S. Life Cycle Inventory and Impact Assessment Data for 2014 Ingeo Polylactide Production. *Ind. Biotechnol.* **2015**, *11* (3), 167–180. https://doi.org/10.1089/ind.2015.0003.

(2) Auras, R.; Harte, B.; Selke, S. An Overview of Polylactides as Packaging Materials. *Macromol. Biosci*. **2004**, *4*(9), 835–864. https://doi.org/10.1002/mabi.200400043.

(3) Nair, L. S.; Laurencin, C. T. Biodegradable Polymers as Biomaterials. *Prog. Polym. Sci.* **2007**, *32*, 762–798. https://doi.org/10.1016/j.progpolymsci.2007.05.017.

(4) Castro-Aguirre, E.; Iñiguez-Franco, F.; Samsudin, H.; Fang, X.; Auras, R. Poly(Lactic Acid)—Mass Production, Processing, Industrial Applications, and End of Life. *Adv. Drug Deliv. Rev*. **2016**, *107*, 333–366. https://doi.org/10.1016/j.addr.2016.03.010.

(5) Drumright, R. E.; Gruber, P. R.; Henton, D. E. Polylactic Acid Technology. *Adv. Mater.* **2000**, *12* (23), 1841–1846. https://doi.org/10.1002/1521-4095(200012)12:23<1841::AID-ADMA1841>3.0.CO;2-E.

(6) Dechy-Cabaret, O.; Martin-Vaca, B.; Bourissou, D. Controlled Ring-Opening Polymerization of Lactide and Glycolide. *Chem. Rev.* **2004**, *104* (12), 6147–6176. https://doi.org/10.1021/cr040002s.

(7) Platel, R. H.; Hodgson, L. M.; Williams, C. K. Biocompatible Initiators for Lactide Polymerization. *Polym. Rev.* **2008**, *48* (1), 11–63. https://doi.org/10.1080/15583720701834166.

(8) Lyubov, D. M.; Tolpygin, A. O.; Trifonov, A. A. Rare-Earth Metal Complexes as Catalysts for Ring-Opening Polymerization of Cyclic Esters. *Coord. Chem. Rev.* **2019**, *392*, 83–145. https://doi.org/10.1016/j.ccr.2019.04.013.

(9) Dijkstra, P. J.; Du, H.; Feijen, J. Single Site Catalysts for Stereoselective Ring-Opening Polymerization of Lactides. *Polym. Chem*. **2011**, *2* 520–527. https://doi.org/10.1039/c0py00204f.

(10) Stanford, M. J.; Dove, A. P. Stereocontrolled Ring-Opening Polymerisation of Lactide. *Chem. Soc. Rev.* **2010**, *39* (2), 486–494. https://doi.org/10.1039/b815104k.

(11) Thomas, C. M. Stereocontrolled Ring-Opening Polymerization of Cyclic Esters: Synthesis of New Polyester Microstructures. *Chem. Soc. Rev*. January **2010**, *39*, 165–173. https://doi.org/10.1039/b810065a.

(12) Kakuta, M.; Hirata, M.; Kimura, Y. Stereoblock Polylactides as High-Performance Bio-Based Polymers. *Polym. Rev.* **2009**, *49* (2), 107–140. https://doi.org/10.1080/15583720902834825.

(13) Tsuji, H. Poly(Lactide) Stereocomplexes: Formation, Structure, Properties, Degradation, and Applications. *Macromol. Biosci.* **2005**, *5* (7), 569–597. https://doi.org/10.1002/mabi.200500062.

(14) Sudesh, K.; Abe, H.; Doi, Y. Synthesis, Structure and Properties of Polyhydroxyalkanoates: Biological Polyesters. *Prog. Polym. Sci*. **2000**, *25*, 1503–1555. https://doi.org/10.1016/S0079-6700(00)00035-6.

(15) Grigore, M. E.; Grigorescu, R. M.; Iancu, L.; Ion, R.-M.; Zaharia, C.; Andrei, E. R. Methods of Synthesis, Properties and Biomedical Applications of Polyhydroxyalkanoates: A Review. *J. Biomater. Sci., Polym. Ed.* **2019**, *30*(9), 695–712. https://doi.org/10.1080/09205063.2019.1605866.

(16) Anjum, A.; Zuber, M.; Zia, K. M.; Noreen, A.; Anjum, M. N.; Tabasum, S. Microbial Production of Polyhydroxyalkanoates (PHAs) and Its Copolymers: A Review of Recent Advancements. *Int. J. Biol. Macromol*. **2016**, *89*, 161–174. https://doi.org/10.1016/j.ijbiomac.2016.04.069.

(17) Cai, C. X.; Amgoune, A.; Lehmann, C. W.; Carpentier, J. F. Stereoselective Ring-Opening Polymerization of Racemic Lactide Using Alkoxy-Amino-Bis(Phenolate) Group 3 Metal Complexes. *Chem. Commun.* **2004**, *4* (3), 330–331. https://doi.org/10.1039/b314030j.

(18) Bonnet, F.; Cowley, A. R.; Mountford, P. Lanthanide Borohydride Complexes Supported by Diaminobis(Phenoxide) Ligands for the Polymerization of ε-Caprolactone and L- and Rac-Lactide. *Inorg. Chem.* **2005**, *44* (24), 9046–9055. https://doi.org/10.1021/ic051316g.

(19) Jaffredo, C. G.; Chapurina, Y.; Kirillov, E.; Carpentier, J. F.; Guillaume, S. M. Highly

Stereocontrolled Ring-Opening Polymerization of Racemic Alkyl β-Malolactonates Mediated by Yttrium [Amino-Alkoxy-Bis(Phenolate)] Complexes. *Chem. Eur. J.* **2016**, *22* (22), 7629–7641. https://doi.org/10.1002/chem.201600223.

(20) Amgoune, A.; Thomas, C. M.; Carpentier, J. F. Controlled Ring-Opening Polymerization of Lactide by Group 3 Metal Complexes. *Pure Appl. Chem.* **2007**; Vol. *79*, 2013–2030. https://doi.org/10.1351/pac200779112013.

(21) Liang, Z.; Ni, X.; Li, X.; Shen, Z. Synthesis and Characterization of Benzoxazine-Functionalized Amine Bridged Bis(Phenolate) Lanthanide Complexes and Their Application in the Ring-Opening Polymerization of Cyclic Esters. *Dalton. Trans.* **2012**, *41* (9), 2812–2819. https://doi.org/10.1039/c2dt11736c.

(22) Duan, Y. L.; He, J. X.; Wang, W.; Zhou, J. J.; Huang, Y.; Yang, Y. Synthesis and Characterization of Dinuclear Rare-Earth Complexes Supported by Amine-Bridged Bis(Phenolate) Ligands and Their Catalytic Activity for the Ring-Opening Polymerization of l-Lactide. *Dalton Trans.* **2016**, *45* (26), 10807–10820. https://doi.org/10.1039/c6dt01486k.

(23) Amgoune, A.; Thomas, C. M.; Roisnel, T.; Carpentier, J. F. Ring-Opening Polymerization of Lactide with Group 3 Metal Complexes Supported by Dianionic Alkoxy-Amino-Bisphenolate Ligands: Combining High Activity, Productivity, and Selectivity. *Chem. Eur. J.* **2006**, *12* (1), 169–179. https://doi.org/10.1002/chem.200500856.

(24) Liu, X.; Shang, X.; Tang, T.; Hu, N.; Pei, F.; Cui, D.; Chen, X.; Jing, X. Achiral Lanthanide Alkyl Complexes Bearing N,O Multidentate Ligands. Synthesis and Catalysis of Highly

Heteroselective Ring-Opening Polymerization of Rac-Lactide. *Organometallics* **2007**, *26* (10), 2747–2757. https://doi.org/10.1021/om0700359.

(25) Nie, K.; Gu, X.; Yao, Y.; Zhang, Y.; Shen, Q. Synthesis and Characterization of Amine Bridged Bis(Phenolate) Lanthanide Aryloxides and Their Application in the Polymerization of Lactide. *Dalton Trans.* **2010**, *39* (29), 6832–6840. https://doi.org/10.1039/c001888k.

(26) Zeng, T.; Qian, Q.; Zhao, B.; Yuan, D.; Yao, Y.; Shen, Q. Synthesis and Characterization of Rare-Earth Metal Guanidinates Stabilized by Amine-Bridged Bis(Phenolate) Ligands and Their Application in the Controlled Polymerization of Rac-Lactide and Rac-β-Butyrolactone. *RSC Adv.* **2015**, *5* (65), 53161–53171. https://doi.org/10.1039/c5ra10151d.

(27) Nie, K.; Fang, L.; Yao, Y.; Zhang, Y.; Shen, Q.; Wang, Y. Synthesis and Characterization of Amine-Bridged Bis(Phenolate)Lanthanide Alkoxides and Their Application in the Controlled Polymerization of Rac-Lactide and Rac-β-Butyrolactone. *Inorg. Chem.* **2012**, *51* (20), 11133–11143. https://doi.org/10.1021/ic301746c.

(28) Ouyang, H.; Nie, K.; Yuan, D.; Yao, Y. Synthesis of Amine-Bridged Bis(Phenolate) Rare-Earth Metal Aryloxides and Their Catalytic Performances for the Ring-Opening Polymerization of l-Lactic Acid: O -Carboxyanhydride and l-Lactide. *Dalton Trans.* **2017**, *46* (45), 15928–15938. https://doi.org/10.1039/c7dt03001k.

(29) Chapurina, Y.; Klitzke, J.; Casagrande, O. D. L.; Awada, M.; Dorcet, V.; Kirillov, E.; Carpentier, J. F. Scandium versus Yttrium{amino-Alkoxy-Bis(Phenolate)} Complexes for the Stereoselective Ring-Opening Polymerization of Racemic Lactide and β-Butyrolactone. *Dalton Trans.* **2014**, *43* (38), 14322–14333. https://doi.org/10.1039/c4dt01206b.

(30) Bouyahyi, M.; Ajellal, N.; Kirillov, E.; Thomas, C. M.; Carpentier, J.-F. F. Exploring Electronic versus Steric Effects in Stereoselective Ring-Opening Polymerization of Lactide and β-Butyrolactone with Amino-Alkoxy-Bis(Phenolate)-Yttrium Complexes. *Chem. Eur. J.* **2011**, *17* (6), 1872–1883. https://doi.org/10.1002/chem.201002779.

(31) Amgoune, A.; Thomas, C. M.; Ilinca, S.; Roisnel, T.; Carpentier, J.-F. Highly Active, Productive, and Syndiospecific Yttrium Initiators for the Polymerization of Racemic β-Butyrolactone. *Angew. Chem., Int. Ed.* **2006**, *45*, 2782–2784. https://doi.org/10.1002/ange.200600058.

(32) Ajellal, N.; Bouyahyi, M.; Amgoune, A.; Thomas, C. M.; Bondon, A.; Pillin, I.; Grohens, Y.; Carpentier, J. F. Syndiotactic-Enriched Poly(3-Hydroxybutyrate)s via Stereoselective Ring-Opening Polymerization of Racemic β-Butyrolactone with Discrete Yttrium Catalysts. *Macromolecules* **2009**, *42* (4), 987–993. https://doi.org/10.1021/ma8022734.

(33) Ligny, R.; Guillaume, S. M.; Carpentier, J. Yttrium-Mediated Ring-Opening Copolymerization of Oppositely Configurated 4-Alkoxymethylene-β-Propiolactones: Effective Access to Highly Alternated Isotactic Functional PHAs. *Chem. Eur. J.* **2019**, *25* (25), 6412–6424. https://doi.org/10.1002/chem.201900413.

(34) Ligny, R.; Hänninen, M. M.; Guillaume, S. M.; Carpentier, J.-F. Highly Syndiotactic or Isotactic Polyhydroxyalkanoates by Ligand-Controlled Yttrium-Catalyzed Stereoselective Ring-Opening Polymerization of Functional Racemic β-Lactones. *Angew. Chem., Int. Ed.* **2017**, *56* (35), 10388–10393. https://doi.org/10.1002/anie.201704283.

(35) Carpentier, J. F. Rare-Earth Complexes Supported by Tripodal Tetradentate Bis(Phenolate)

Ligands: A Privileged Class of Catalysts for Ring-Opening Polymerization of Cyclic Esters. *Organometallics* **2015**, *34* (17), 4175–4189. https://doi.org/10.1021/acs.organomet.5b00540.

(36) Amgoune, A.; Thomas, C. M.; Carpentier, J.-F. F. Yttrium Complexes as Catalysts for Living and Immortal Polymerization of Lactide ToHighly Heterotactic PLA. *Macromol. Rapid Commun.* **2007**, *28* (6), 693–697. https://doi.org/10.1002/marc.200600862.

(37) Zhao, W.; Wang, Y.; Liu, X.; Cui, D. Facile Synthesis of Fluorescent Dye Labeled Biocompatible Polymers via Immortal Ring-Opening Polymerization. *Chem. Commun.* **2012**, *48* (37), 4483–4485. https://doi.org/10.1039/c2cc31061a.

(38) Zhao, W.; Li, C.; Liu, B.; Wang, X.; Li, P.; Wang, Y.; Wu, C.; Yao, C.; Tang, T.; Liu, X.; et al. A New Strategy to Access Polymers with Aggregation-Induced Emission Characteristics. *Macromolecules* **2014**, *47* (16), 5586–5594. https://doi.org/10.1021/ma500985j.

(39) Stirling, E.; Champouret, Y.; Visseaux, M. Catalytic Metal-Based Systems for Controlled Statistical Copolymerisation of Lactide with a Lactone. *Polym. Chem*. **2018**, *9*(19), 2517–2531. https://doi.org/10.1039/c8py00310f.

(40) Abe, H.; Doi, O.; Hori, Y.; Hagiwara, T. Physical Properties and Enzymatic Degradability of Copolymers of (R)-3-Hydroxybutyric Acid and (S,S)-Lactide. *Polymer* **1998**, *39* (1), 59–67. https://doi.org/10.1016/S0032-3861(97)00240-1.

(41) Liu, L.; Wei, Z. Y.; Qi, M. Synthesis and Characterization of Biodegradable Aliphatic Polyesters Using Dibutylmagnesium as Initiator. *Chinese Chem. Lett.* **2007**, *18* (6), 744–

746. https://doi.org/10.1016/j.cclet.2007.04.011.

(42) Cross, E. D.; Allan, L. E. N.; Decken, A.; Shaver, M. P. Aluminum Salen and Salan Complexes in the Ring-Opening Polymerization of Cyclic Esters: Controlled Immortal and Copolymerization of Rac -β-Butyrolactone and Rac -Lactide. *J. Polym. Sci. Part A, Polym. Chem.* **2013**, *51* (5), 1137–1146. https://doi.org/10.1002/pola.26476.

(43) Fagerland, J.; Finne-Wistrand, A.; Pappalardo, D. Modulating the Thermal Properties of Poly(Hydroxybutyrate) by the Copolymerization of: Rac -β-Butyrolactone with Lactide. *New J. Chem.* **2016**, *40* (9), 7671–7679. https://doi.org/10.1039/c6nj00298f.

(44) García-Valle, F. M.; Tabernero, V.; Cuenca, T.; Mosquera, M. E. G.; Cano, J.; Milione, S. Biodegradable PHB from Rac- β-Butyrolactone: Highly Controlled ROP Mediated by a Pentacoordinated Aluminum Complex. *Organometallics* **2018**, *37* (6), 837–840. https://doi.org/10.1021/acs.organomet.7b00843.

(45) García-Valle, F. M.; Cuenca, T.; Mosquera, M. E. G.; Milione, S.; Cano, J. Ring-Opening Polymerization (ROP) of Cyclic Esters by a Versatile Aluminum Diphenoxyimine Complex: From Polylactide to Random Copolymers. *Eur. Polym. J.* **2020**, *125*, 109527. https://doi.org/10.1016/j.eurpolymj.2020.109527.

(46) Jeffery, B. J.; Whitelaw, E. L.; Garcia-Vivo, D.; Stewart, J. A.; Mahon, M. F.; Davidson, M. G.; Jones, M. D. Group 4 Initiators for the Stereoselective ROP of Rac-β-Butyrolactone and Its Copolymerization with Rac-Lactide. *Chem. Commun.* **2011**, *47* (45), 12328–12330. https://doi.org/10.1039/c1cc15265c.

(47) Aluthge, D. C.; Xu, C.; Othman, N.; Noroozi, N.; Hatzikiriakos, S. G.; Mehrkhodavandi, P.

PLA-PHB-PLA Triblock Copolymers: Synthesis by Sequential Addition and Investigation of Mechanical and Rheological Properties. *Macromolecules* **2013**, *46* (10), 3965–3974. https://doi.org/10.1021/ma400522n.

(48) Yu, I.; Ebrahimi, T.; Hatzikiriakos, S. G.; Mehrkhodavandi, P. Star-Shaped PHB-PLA Block Copolymers: Immortal Polymerization with Dinuclear Indium Catalysts. *Dalton Trans.* **2015**, *44* (32), 14248–14254. https://doi.org/10.1039/c5dt02357b.

(49) Gruszka, W.; Walker, L. C.; Shaver, M. P.; Garden, J. A. In Situ Versus Isolated Zinc Catalysts in the Selective Synthesis of Homo and Multi-Block Polyesters. *Macromolecules* **2020**, *53* (11), 4294–4302. https://doi.org/10.1021/acs.macromol.0c00277.

(50) Whitehorne, T. J. J.; Schaper, F. Lactide, β-Butyrolactone, δ-Valerolactone, and ε-Caprolactone Polymerization with Copper Diketiminate Complexes. *Can. J. Chem.* **2014**, *92* (3), 206–214. https://doi.org/10.1139/cjc-2013-0392.

(51) Kramer, J. W.; Treitler, D. S.; Dunn, E. W.; Castro, P. M.; Roisnel, T.; Thomas, C. M.; Coates, G. W. Polymerization of Enantiopure Monomers Using Syndiospecific Catalysts: A New Approach to Sequence Control in Polymer Synthesis. *J. Am. Chem. Soc.* **2009**, *131* (44), 16042–16044. https://doi.org/10.1021/ja9075327.

(52) Ligny, R.; Hänninen, M. M.; Guillaume, S. M.; Carpentier, J. F. Steric vs. Electronic Stereocontrol in Syndio- or Iso-Selective ROP of Functional Chiral β-Lactones Mediated by Achiral Yttrium-Bisphenolate Complexes. *Chem. Commun.* **2018**, *54* (58), 8024–8031. https://doi.org/10.1039/c8cc03842b.

(53) Fadlallah, S.; Jothieswaran, J.; Capet, F.; Bonnet, F.; Visseaux, M. Frontispiece: Mixed

Allyl Rare-Earth Borohydride Complexes: Synthesis, Structure, and Application in (Co-)Polymerization Catalysis of Cyclic Esters. *Chem. Eur. J.* **2017**, *23* (62). https://doi.org/10.1002/chem.201786264.

(54) Nomura, N.; Akita, A.; Ishii, R.; Mizuno, M. Random Copolymerization of ε-Caprolactone with Lactide Using a Homosalen-Al Complex. *J. Am. Chem. Soc.* **2010**, *132* (6), 1750–1751. https://doi.org/10.1021/ja9089395.

(55) Shi, T.; Luo, W.; Liu, S.; Li, Z. Controlled Random Copolymerization of Rac -Lactide and ε -Caprolactone by Well-Designed Phenoxyimine Al Complexes. *J. Polym. Sci. Part A, Polym. Chem.* **2018**, *56* (6), 611–617. https://doi.org/10.1002/pola.28932.

(56) Zell, M. T.; Padden, B. E.; Paterick, A. J.; Thakur, K. A. M.; Kean, R. T.; Hillmyer, M. A.; Munson, E. J. Unambiguous Determination of the 13C and 1H NMR Stereosequence Assignments of Polylactide Using High-Resolution Solution NMR Spectroscopy. *Macromolecules* **2002**, *35* (20), 7700–7707. https://doi.org/10.1021/ma0204148.

(57) Thakur, K. A. M.; Kean, R. T.; Hall, E. S.; Kolstad, J. J.; Lindgren, T. A.; Doscotch, M. A.; Siepmann, J. I.; Munson, E. J. High-Resolution 13C and 1H Solution NMR Study of Poly(Lactide). *Macromolecules* **1997**, *30* (8), 2422–2428. https://doi.org/10.1021/ma9615967.

(58) Kasperczyk, J. E. HETCOR NMR Study of Poly(Rac-Lactide) and Poly(Meso-Lactide). *Polymer* **1999**, *40* (19), 5455–5458. https://doi.org/10.1016/S0032-3861(99)00128-7.

(59) Kemnitzer, J. E.; McCarthy, S. P.; Gross, R. A. Syndiospecific Ring-Opening Polymerization of β-Butyrolactone To Form Predominantly Syndiotactic Poly(β-

Hydroxybutyrate) Using Tin(IV) Catalysts. *Macromolecules* **1993**, *26* (23), 6143–6150. https://doi.org/10.1021/ma00075a001.

(60) Chile, L. E.; Mehrkhodavandi, P.; Hatzikiriakos, S. G. A Comparison of the Rheological and Mechanical Properties of Isotactic, Syndiotactic, and Heterotactic Poly(Lactide). *Macromolecules* **2016**, *49* (3), 909–919. https://doi.org/10.1021/acs.macromol.5b02568.

(61) Fox, T. G. Influence of Diluent and of Copolymer Composition on the Glass Temperature of a Polymer System. *Bull. Am. Phys. Soc.* **1956**, *1*, 123.

(62) Fineman, M.; Ross, S. D. Linear Method for Determining Monomer Reactivity Ratios in Copolymerization. *J. Polym. Sci.* **1950**, *5* (2), 259–262. https://doi.org/10.1002/pol.1950.120050210.

(63) Kelen, T.; TÜdÕs, F. Analysis of the Linear Methods for Determining Copolymerization Reactivity Ratios. I. A New Improved Linear Graphic Method. *J. Macromol. Sci., Part A: Chem.* **1975**, *9* (1), 1–27. https://doi.org/10.1080/00222337508068644.

(64) Beckingham, B. S.; Sanoja, G. E.; Lynd, N. A. Simple and Accurate Determination of Reactivity Ratios Using a Nonterminal Model of Chain Copolymerization. *Macromolecules* **2015**, *48* (19), 6922–6930. https://doi.org/10.1021/acs.macromol.5b01631.

(65) Tabata, Y.; Abe, H. Synthesis and Properties of Alternating Copolymers of 3-Hydroxybutyrate and Lactate Units with Different Stereocompositions. *Macromolecules* **2014**, *47* (21), 7354–7361. https://doi.org/10.1021/ma501783f.

(66) Herrmann, W. A.; Munck, F. C.; Artus, G. R. J.; Runte, O.; Anwander, R. 1,3-

Dimethylimidazolin-2-Ylidene Carbene Donor Ligation in Lanthanide Silylamide Complexes. *Organometallics* **1997**, *16* (4), 682–688. https://doi.org/10.1021/om9607715.